Feasibility of Diffusion Tensor Imaging at 0.5T

Curtis N Wiens[1], Chad T Harris[1], Andrew T Curtis[1], Philip J Beatty[1], and Jeff A Stainsby[1]
[1]Research and Development, Synaptive Medical, Toronto, ON, Canada

Synopsis

This work examined the feasibility of diffusion tensor imaging (DTI) at 0.5T, a technique performed almost exclusively at field strengths of at least 1.5T. 2D diffusion-weighted axial spin-echo echo-planar imaging and 3D T1 weighted acquisitions were performed in the NIST isotropic diffusion phantom, a DTI phantom, and 5 healthy volunteers on a head-specific 0.5T MRI system. ADC measurements of the NIST phantom were in excellent agreement with previously recorded 3T measurements while DTI processing and tractography performed using Modus Plan was successful in all of the volunteers.

Introduction

Diffusion tensor imaging (DTI) is emerging as an important tool for the pre-operative planning of neurosurgery[1]. Incorporation of DTI into neurosurgery has been shown to offer many benefits including: reduced surgery durations, reduced prevalence of seizures during surgery, improved surgical outcomes, and improved post-operative survival[2,3]. Lower field strengths offer several advantages for neurosurgical planning using DTI. The reduction in geometric distortions at lower field strengths result in improved spatial accuracy of fiber tracts. Furthermore, a lower field strength offers a more compact system with less weight and a more compact fringe field which could improve accessibility. Despite these advantages, evaluations of DTI at field strengths below 1.5T is extremely limited[4]. In this work, we leveraged the high-performance gradient set of a small footprint, head-only MR system[5] to demonstrate the feasibility of performing DTI at 0.5T.

Methods

All imaging was performed on a head-specific 0.5T MR system equipped with a 16 channel head coil[5]. This system contains a high-performance gradient set with a maximum gradient strength and slew rate of 100mT/m and 400T/m/s per axis respectively.

NIST Isotropic Diffusion Phantom: 2D diffusion-weighted spin-echo echo-planar imaging (diffusion EPI) were performed on a quantitative diffusion phantom (High Precision Devices, Boulder, CO). Parameters for the DTI acquisition were: in-plane resolution: 1.1x1.1mm, slices =1, slice thickness = 5.0mm, b-value = 800mm/s^2, diffusion directions=24 (plus 4 b=0), TR=15s, TE=139ms, acceleration factor = 2, averages=2, acquisition time = 14min. In accordance with their guidelines, the phantom was filled with ice-water at 0°C to account for the temperature dependence of ADC measurements. ADC measurements of were made by computing the mean value throughout a circular region of interest within each vial.

DTI Phantom: Diffusion EPI and 3D gradient echo acquisitions was performed on a DTI phantom previously described by Whitton et al[6]. This phantom consists of flexible fiber bundles with complex geometries including curved, kissing, and interweaving. Parameters for the diffusion acquisition were: in-plane resolution: 3.0x3.0mm, slice thickness = 3.0mm, b-value = 800mm/s^2, diffusion directions=60 (plus 8 b=0), TR=4.5s, TE=69ms, acceleration factor = 2, averages=2, acquisition time = 10.3min. 3D gradient echo acquisition parameters: resolution=1.1x1.1x1.1, flip angle = 26°, TR = 11.2ms, TE =5.2ms.

In vivo: Diffusion EPI and 3D gradient echo acquisitions were performed on 5 healthy volunteers with informed consent in compliance with health and safety protocols. Parameters for the diffusion acquisition were: in-plane resolution: 2.4x2.4mm, slice thickness = 3.0mm, b-value = 800mm/s^2, diffusion directions=52 (plus 8 b=0), TR=5.3s, TE=79ms, averages=2, acceleration factor = 2, acquisition time = 10.6min. 3D gradient echo with the following parameters: Resolution=1.1x1.1x1.1, Flip Angle = 26°, TR = 11.2ms, TE =5.2ms.

Reconstruction: Diffusion encoded images, apparent diffusion coefficient (ADC) and fractional anisotropy (FA) maps were reconstructed from the DTI acquisitions, correcting for gradient non-linearities[7] and performing joint denoising processing[8,9]. In addition, fiber tractography was computed using Modus Plan^{TM} (Synaptive Medical, Toronto). This software performed image registration of DTI and T1 weighted images and fiber tract creation and segmentation.

Results

Figure 1 shows a PVP concentration schematic (a), ADC maps (b) and measured and literature ADC values of the NIST isotropic diffusion phantom. Good agreement between ADC values was demonstrated between our measurements at 0.5T and previous measurements made at 3.0T[10].

Schematics of the DTI phantom are shown in Figure 2a. Figure 2b shows tractography overlaid on T1-weighted images for curved and interweaving fiber orientations. For each orientation, excellent alignment between the tracts and the anatomical images is observed.

Figure 3 shows representative diffusion encoded images of one subject. Figure 4 shows the ADC, FA, and RGB of a center cut axial slice across all 5 volunteers. Figure 5 shows tractography results for one of the subjects.

Discussion

The ADC values obtained using the NIST isotropic diffusion phantom were in good agreement with results obtained in a multi-center study at 3T. This is a promising result that indicates that a 0.5T scanner can be used to obtain ADC measurements consistent with higher field systems. However, further investigation would need to be done to understand how measurement consistency at 0.5T compares to the consistency observed in higher field systems.

A small pilot study involving 5 healthy volunteers was performed to further demonstrate feasibility. In this study, fat saturation preparation pulses were not applied as lower field strength results in a less drastic chemical shift artifact. The combination of strong gradients and no fat saturation allowed for improved sampling efficiency when compared to higher field systems, partially alleviating some of the SNR constraints of a mid-field system.

Conclusions

Phantom and in-vivo results demonstrated that Diffusion Tensor Imaging can be successfully performed at 0.5T and used 1) to compute high quality ADC, FA and RGB maps and 2) by tractography software for fiber tractography and white matter segmentation.

Acknowledgements

References

1. Essayed WI, Zhang F, Unadkat P, Cosgrove GR, Golby AJ, O'Donnell LJ. White matter tractography for neurosurgical planning: A topography-based review of the current state of the art. NeuroImage: Clinical. 2017;15:659-672.

2. Bello L, Gambini A, Castellano A, Carrabba G, Acerbi F, Fava E, Giussani C, Cadioli M, Blasi V, Casarotti A, Papagno C, Gupta AK, Gaini S, Scotti G, Falini A. Motor and language DTI Fiber Tracking combined with intraoperative subcortical mapping for surgical removal of gliomas, NeuroImage , 2008.

3. Romano A, D'Andrea G, Minniti G, Mastronardi L, Ferrante L, Fantozzi LM, Bozzao A. Pre-surgical planning and MR-tractography utility in brain tumour resection. Eur. Radiol. , 2009.

4. Hori M, Okubo T, Aoki S, Kumagai H, Ariki T. Line scan diffusion tensor MRI at low magnetic field strength: Feasibility study of cervical spondylotic myelopathy in an early clinical stage. Journal of Magnetic Resonance Imaging. 2006;23:183-188.

5. Panther A, Thevathasen G, Connell IRO, Yao Y, Wiens CN, Curtis AT, Bindseil GA, Harris CT, Beatty PJ, Stainsby JA, Cunningham CH, Chronik BA, Piron C. A Dedicated Head-Only MRI Scanner for Point-of-Care Imaging. Proceedings of the 27th Annual Meeting of ISMRM. Montreal, Canada, 2019. Abstract 3679.

6. Whitton G, Gmeiner T, Harris CT, Kerins F. A novel diffusion tensor imaging phantom that simulates complex neuro-architecture for potential validation of DTI processing. Proceedings of the 24th Annual Meeting of ISMRM. Singapore. Abstract 3061.

7. Bammer R, Markl M, Barnett A, Acar B, Alley MT, Pelc NJ, Glover GH, Moseley ME. Analysis and generalized correction of the effect of spatial gradient field distortions in diffusion-weighted imaging. Magnetic Resonance in Medicine. 2003;50(3):560-569.

8. Manjon JV, Coupe P, Concha L, Buades A, Collins DL Robles M. Diffusion Weighted Image Denoising Using Overcomplete Local PCA. PLoS ONE 8(9): e73021.

9. Veraart J, Novikov DS, Christiaens D, Ades-aron B, Sijbers J, Fieremans E. Denoising of diffusion MRI using random matrix theory. Neuroimage. 2016 November 15; 142: 394-406.

10. Palacios EM, Martin AJ, Boss MA, Ezekiel F, Chang YS, Yuh EL, Vassar MJ, Schnyer DM, MacDonald CL, Crawford, KL, Irimia A, Toga AW, Mukherjee P, TRACK-TBI Investigators. Towards Precision and Reproducibility of Diffusion Tensor Imaging: A Multicenter Diffusion Phantom and Traveling Volunteer Study. Am J Neuroradiol. 2017; 38(3):537-545.
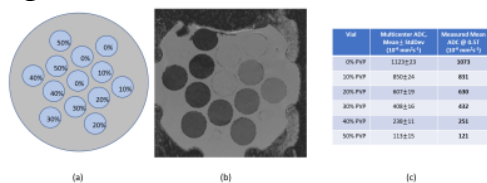
Figures

Figure 1: NIST Isotropic Diffusion Phantom Results. (a) Labels of percentage PVP by vial. (b) Reconstructed ADC map from 0.5T scanner. (c) Measured ADC values compared to published multicenter ADC values[10]. Multicenter ADC values show mean and standard deviation across 13 3T scanners across 3 vendors.
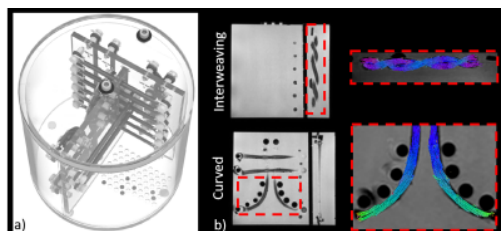

Figure 2: A DTI phantom containing flexible fiber bundles demonstrates the feasibility of imaging complex geometries with excellent geometric alignment. a) Schematic of the DTI phantom. b) Zoomed in tractography overlaid on T1 weighted images are shown of curved and interweaving fibers.
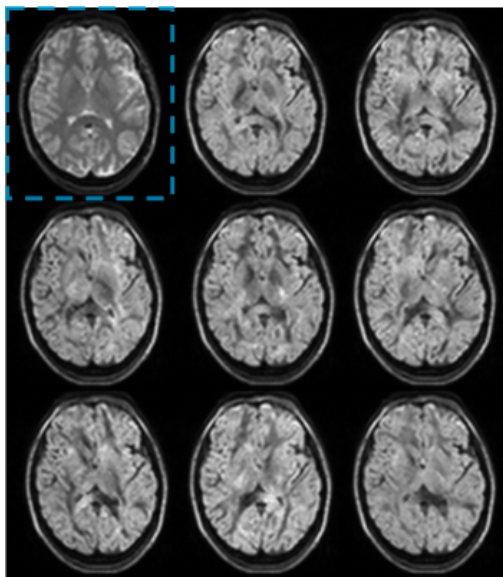
Figure 3: Representative diffusion encoded images. The b-value=0 (blue box) and 8 of 52 b-value=800mm/s^2 diffusion encoded images are shown.
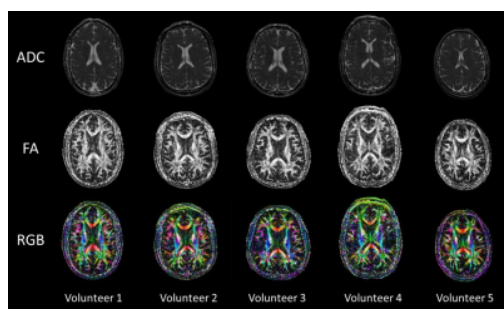

Figure 4: ADC, FA, and RGB maps from a center cut axial slice of each volunteer show that DTI imaging at 0.5T is feasible.
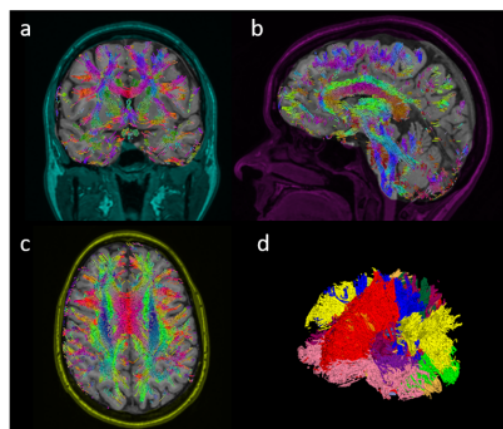

Figure 5: Tractography and white matter segmentation of a representative volunteer. Coronal (a), sagittal (b), and axial (c) tractography overlaid on a 3D T1 weighted data set and white matter segmentation (d) are shown.